Journal of Taibah University Medical Sciences (2023) 18(5), 1076–1086

Taibah University

Journal of Taibah University Medical Sciences

www.sciencedirect.com

Original Article

In vitro bio-characterization of solid lipid nanoparticles of favipiravir in A549 human lung epithelial cancer cells

Alaa S. Tulbah, Ph.D.

Pharmaceutics Department, College of Pharmacy, Umm Al Qura University, Makkah, KSA

Received 28 July 2022; revised 8 January 2023; accepted 27 February 2023; Available online 10 March 2023

المخلص

أهداف البحث: يعد سرطان الرئة أحد الأسباب الرئيسية للوفيات في جميع أنحاء العالم. وجد لعلاج فعال علىسرطان الرئة ، قد تكون الجسيمات النانوية الدهنية الصلبة تعتبر الطريقة الفعالة لإيصال الدواء لأن الدواء يمكن أن يصل إلى موقع التأثير ويحسن كفاءة الاستنشاق والترسيب الرئوي. هذه الورقة البحثية تركز على تقييم الجسيمات النانوية الدهنية الصلبة من علاج الفافيبيرافير من حيث قياس مدى فعاليتة على سرطان الرئة من خلال مساعدة الدواء في الوصول إلى موقع التأثير.

طرق البحث: تم استخدام طريقة التبخير الساخن لتطويرالتركيبة النانوية الدوائية من علاج الفافيبيرافير. تم تقييم قابلية بقاء الخلايا المختبرية، ومضادات السرطان ونشاط الامتصاص الخلوي لتركيبة فافيبيرافير على خلايا سرطانية الغدة الرئوية البشرية أ-549.

النتائج: تمت تطوير التركيبة الدوائية من علاج الفافيبيرافير بنجاح. الأهم من ذلك، لوحظ أن تركيبة الفافيبيرافير آمنة وغير سامة في المختبر على خلايا أ-549 بتركيز 322.6 ميكروغرام / مل. كان للتركيبة تأثير مذهل فيما يتعلق بالخصائص المضادة للتكاثر من خلال زيادة طور ج2 / م و ج0 / ج1 من مجموعة الخلايا بمقدار 1.20 و 1.13 مرة، على التوالي ، مقارنة با الخلايا غير المعالجة. بالإضافة إلى ذلك، ساعد العلاج باستخدام فافيبيرافير بشكل كبير في حدوث مرحلة النخر في خلايا أ-549. علاوة على ذلك، فإن استخدام تركيبة فافيبيرافير عزز امتصاص الدواء في الضامة بنسبة 1.23 مرة ، مقارنة بالتركيبة الخالية من المادة الفعالة.

الاستنتاجات: أكدت نتائج البحث أن للتركيبة النانونية من علاج الفافيبيرافير تأثير فعال على خلايا السرطان الرئوية- أ-549. و يشير هذا إلى أنه يمكن استخدام تركيبة الفافيبيرافير كعلاج لسرطان الرئة اللوصول إلى موقع التأثير في الرئتين.

الكلمات المفتاحية: خلايا أ-549؛ السمية الخلوية؛ توزيع دورة الخلية؛ فافيبيرافير؛ التنخر؛ الجسيمات النانوية

Abstract

Objectives: Lung cancer is a leading cause of mortality worldwide. In lung cancer treatment, nebulized solid lipid nanoparticles may be a viable drug delivery method, helping the drug reach sites of action, and improving its inhalation efficiency and pulmonary deposition. This research focused on evaluating the effectiveness of solid lipid nanoparticles of favipiravir (Fav-SLNps) in facilitating drug delivery to sites of action in lung cancer treatment.

Methods: The hot-evaporation method was used to formulate Fav-SLNps. The in vitro cell viability, anticancer effects, and cellular uptake activity were evaluated in A549 human lung adenocarcinoma cells treated with the Fav-SLNp formulation.

Results: The Fav-SLNps were formulated successfully. Importantly, Fav-SLNps at a concentration of 322.6 μg/ml were found to be safe and non-toxic toward A549 cells in vitro. The formulation had potential anti-proliferative properties via increasing the proportions of cells in G2/M and G0/G1 phases to 1.20 and 1.13 times those in untreated cells. Additionally, Fav-SLNp treatment significantly induced necrosis in A549 cells. Furthermore, the use of SLNps in the Fav formulation resulted in a macrophage drug uptake 1.23 times that of the free drug.

Conclusion: Our results confirmed the internalization and anti-cancer activity of the Fav-SLNp formulation in the A549 lung cancer cell line. Our findings suggest that Fav-SLNps could potentially be used as lung cancer treatment to facilitate drug delivery to sites of action in the lungs.

Keywords: A549 cells; Cell cycle distribution; Cytotoxicity; Favipiravir; Nanoparticles; Necrosis

E-mail: astulbah@uqu.edu.sa

Peer review under responsibility of Taibah University.

ELSEVIER Production and hosting by Elsevier

 https://doi.org/10.1016/j.jtumed.2023.02.014

Introduction

Lung cancer is a leading cause of mortality worldwide.[1,2] Recently, its incidence has increased because of smoking and environmental pollution.[3] Surgery, radiation therapy, and chemotherapy are used in lung cancer treatment,[4] and current chemotherapies are delivered through conventional oral or intravenous routes.[5] However, the possibility of inhaled drug delivery has attracted substantial attention in lung cancer treatment because it overcomes several current limitations of chemotherapy, including the targeting of normal cells alongside the inhibition of cancer cell growth.

The use of nanotechnology systems has excellent prospects for therapy development, because it facilitates passive targeting of drugs to tumours, thereby increasing retention and permeability, and enhancing the pharmacokinetic/pharmacodynamic properties of drugs.[6,7,7] Many drug carriers have been used in recent years, e.g., polymers, liposomes, and solid lipid nanoparticles (SLNps), because of their considerable benefits in treating lung cancer, increasing drug stability, and avoiding severe adverse effects.[8–15] In particular, SLNp formulations have been used in many studies and have exhibited good performance in overcoming drug limitations.[16,17]

SLNps are colloidal particles composed of a biocompatible and biodegradable lipid with spherical bilayer vesicles of multiple types: (1) large unilamellar vesicles, (2) multilamellar vesicles, (3) giant unilamellar vesicles, and (4) small unilamellar vesicles.[18] Furthermore, the FDA has approved the use of biodegradable lipid polymers as nanocarriers to increase the solubility and stability of medication, and decrease high drug loading and preparation costs.[17,19,20] The bioavailability and cellular absorption of some poorly water-soluble drugs can be improved through formulation with SLNp nanocarriers.[21,22] For example, Favipiravir (Fav) has been fabricated with solid lipid nanoparticles (SLNs)[19] and has been found to be a promising method for targeted inhalation delivery.[23] The inhalation route, such as through nebulizers, can increase local pulmonary drug concentrations, avoid first-pass metabolism, and decrease systemic adverse effects.[24–27] Nebulization of a drug can convert liquids into aerosols with very small droplets that can reach deep into lung tissue.[9,28,29,28,30] Therefore, new or alternative medicines that can be delivered in this manner with high effectiveness could potentially be used for local lung cancer treatment.

Fav is a purine nucleoside analogue and ribonucleic acid (RNA)-dependent RNA polymerase competitive inhibitor,[19,31–33] which has been used as an anti-viral treatment for influenza[34] and the Ebola virus.[35] Kim et al.[37] have found that Fav therapy on Zika-virus-infected human neural progenitor cells decreases cell killing, increases the phosphorylation of AKT (also known as protein kinase B), and elevates the expression of anti-apoptotic protein B cell lymphoma 2.[36] Another study by Tanaka et al.[37] has indicated that Fav suppresses the viral load in the lungs and produces tumour necrosis factor-α in the airways in infected mice.[37] Extensive research has evaluated the anti-viral effect of Fav[19,34–37] in the lungs. However, because of a lack of studies on the biological effects of Fav on lung cancer cells, this study was aimed at assessing the cytotoxicity, proliferation, necrosis, autophagy properties, and cellular uptake of Fav nanoparticles by using a solid lipid formula (Fav-SLNps) in an A549 cell model.

Materials and Methods

Materials

Chloroform, methanol, and Tween 80 were purchased from Thermo Fisher Inc. (Pittsburgh, PA, USA). Glyceryl behenate (compritol 888) dimethyl sulfoxide, sulforhodamine B (SRB), and Fav were purchased from Sigma Aldrich (MO, USA).

The A549 lung cancer cell line was obtained from the American Type Culture Collection (Rockville, USA). Cell culture materials consisting of phenol red, Dulbecco's modified Eagle's medium, foetal bovine serum, and penicillin/streptomycin were obtained from Corning (MO, USA). The tetrazolium dye (WST-1) test used was purchased from Abcam® (ab155902 WST-1 Cell Proliferation Reagent, USA).

Preparation of the formulation

The SLNps were generated through a hot-evaporation approach, as described by Tulbah and Lee.[19] Briefly, compritol 888 (200 mg) was suspended in chloroform (10 ml), and 20 mg of Fav was suspended in methanol (5 ml). A rotary evaporator was used to evaporate the organic solvents at 72 °C and 150 rpm.

Lipid-drug film was mixed (HG-15D, Homogenizer, Korea) at 15,000 rpm and 70 °C for half an hour with 1.5% (w/v) Tween 80 (10 ml) in the hot surfactant. Subsequently, the mixture was cooled on ice with constant stirring to reach a temperature of 20 °C. Control SLNps without Fav were produced in the same manner.

Evaluation of particle size, polydispersity index, and zeta potential

Dynamic light scattering was applied to evaluate the polydispersity index, zeta potential, and particle size of Fav-SLNps (Zetasizer Nano ZN, Malvern Analytical Ltd., UK). At 25 °C, samples were tested after being diluted in ultra-purified water.

High-performance liquid chromatography (HPLC)

A Waters 996 photodiode array detector was used for HPLC (Waters 2690 Alliance, Shimadzu, Japan) with an Xterra C-18 column (4.6 × 250 mm and 5 m particle size) to quantify Fav. The mobile phase was 5:95 v/v acetonitrile:-water and 0.1% phosphoric acid. The ultraviolet light detector's wavelength, flow rate, and sample injection were set at 320 nm, 1 ml/min, and 10 µl, respectively. A 0.22 µm

syringe filter was used to purify the samples. The sample's retention time was 9.5, minutes and the running time was 13 min.

In vitro aerosol deposition analysis

The Fav-SLNp formula was nebulized with a chilled Andersen MKII Cascade Impactor (ACI, Copley Scientific, UK) in conjunction with a jet nebulizer (VixOne, AZ, USA). Every component of the ACI was washed with a mix of mobile phases and allowed to dry.[19,38] After the ACI plates had been placed at 5 °C in a refrigerator for 60 min to cool,[39] they were used immediately. After completion of 1 h of testing, an electronic digital flow meter was adjusted at a 15 L/min flow rate. The T-piece of the jet nebulizer was then rapidly connected to the ACI induction port. The jet nebulizer reservoir was loaded with 2 ml of the Fav-SLNp formulation (200 μg/ml). As indicated by Pharmacopeia,[40,41] three determinations were performed (n = 3). Methanol (20% v/v) was used to clean the nebulizer's reservoir chamber, ACI plates, adaptors, and filter. The quantity of Fav in each stage was analysed by HPLC. The mass median aerodynamic diameter (MMAD), fine particle dose, geometric standard deviation (GSD), and fine particle fraction (FPF) were determined through Copley inhaler analysis (Copley Scientific, UK), and testing data software impactor recordings.

In vitro bio-characterization

Cell culture

A549 human lung adenocarcinoma cells were maintained in Dulbecco's modified Eagle's medium with 100 mg/mL of penicillin/streptomycin and 10% foetal bovine serum. At 37 °C, the cells were cultured in a 5% CO_2 humidified incubator until confluency was achieved, as recommended by the ATCC.[42–44]

Cell viability and cytotoxicity determination

The SRB test allowed for rapid and accurate assessment of the drug's effects on cell viability in cell culture. The cell viability after treatment with the Fav-SLNp formula and free Fav was assessed in lung cells, as previously described.[45,46] The SRB test was used to evaluate drug cytotoxicity immediately and precisely in cell culture samples. A549 lung adenocarcinoma cells were used to test the cytotoxicity of the Fav-SLNps and free Fav, as previously described.[45,46] In brief, 100 μL, 5×10^3 of cell suspension was added and cultured in 96-well plates for 1 day in complete medium. Subsequently, Fav-SLNps and or Fav (0.3–1000 μg/mL) was added to the cells; after 3 days of exposure, the medium was replaced with 150 μL of 10% trichloroacetic acid and incubated for 1 h at 4 °C to fix the cells. The cells were then rinsed with distilled water and incubated for 10 min with SRB solution (0.4%) at 25 °C. The plates were rinsed three times with acetic acid (1%). Tris-based solution (150 μL, 10 mM) was used to dissolve the protein-bound SRB stain. A microplate reader (BMG LABTECH®-FLUOstar, Omega, Germany) was subsequently used to determine the transmission density at 540 nm. According to the preceding descriptions,[14,44,47,48] cell viability was revealed by assessment of the percentage of viable cells in the untreated control group. The IC_{50} was defined as the concentration that decreased cell viability to 50% that of untreated cells.[9] The IC_{50} estimates were determined by calculation of the cell viability percentage versus concentration (μg/mL).

Assessment of cell cycle distribution

To estimate the effects of the Fav-SLNp formula on the cell cycle distribution, we treated the A549 human lung adenocarcinoma cell model with 300 μg/mL of the compound for as long as 1 day. Cells (10^5 cells) were trypsinized and rinsed twice with chilled buffer (PBS, pH 7.4), as previously described.[49,50] The cells were re-suspended in 2 ml of 60% chilled ethanol for 1 h during fixation; rinsed twice with buffer (PBS, pH 7.4); and then re-suspended in 1 ml of PBS containing 50 μg/mL of RNase A and 10 μg/mL of propidium iodide (PI). Flow cytometry analysis was performed with an FL2 (λex/em 535/617 nm) signal indicator (ACEA NovocyteTM flow cytometer, ACEA Biosciences Inc., CA, USA) for 20 min at 37 °C for deoxyribonucleic acid (DNA) content evaluation. A total of 12,000 events were collected for each sample. ACEA NovoExpressTM software was used to calculate the percentage of cells in each cell cycle phase. Each dose was tested three times, and the data reflect the mean ± SD of the three replicates.

Apoptosis evaluation

An apoptosis detection kit with calcium-dependent phospholipid-binding protein V-FITC (Abcam Inc., Cambridge Science Park, Cambridge, UK), and flow cytometry with two fluorescence channels was used to examine the effects of the Fav-SLNp formulation on programmed cells death (necrosis/apoptosis cell populations), as previously described.[49–51] Briefly, A549 human lung adenocarcinoma cells were treated with 300 μg/mL of the Fav-SLNp formula. After 1 day of treatment at the compound's predetermined IC_{50s}, trypsinization was performed to detach the cells. The cells were then rinsed twice with chilled PBS, pH 7.4, buffer and kept in the dark for 30 min at room temperature with a solution of Annexin V-FITC/PI (0.5 ml), as directed by the manufacturer. After labelling, cells were inserted into an ACEA NovocyteTM flow cytometer, and the FL1&2 indicator detector (λex/em 535/617 nm for PI and λex/em 488/530 nm for FITC) was used to detect FITC and PI fluorescence. In total, 12,000 signals were recorded for each examination, and cells positive for PI and/or FITC were counted through quadrant inspection in ACEA NovoExpressTM.

Autophagy evaluation

A dye (acridine orange lysosomal) was applied in conjunction with flow cytometric analysis to quantify autophagic cell death, as previously described.[49,50] Fav-SLNps (300 μg/mL) were used to treat A549 human lung adenocarcinoma cells for 24 h; the cells were then trypsinized and rinsed twice with chilled pH 7.4 PBS buffer. Acridine orange (10 M) was used to dye the cells, which were then incubated for 30 min in the dark at 37 °C. After labelling, the cells were injected into an ACEA NovocyteTM flow cytometer, and the acridine orange fluorescent indicator was evaluated according to the FL1 signal (λex/em 488/530 nm). For each test,

12,000 signals were recorded, and the net fluorescence intensity was measured in ACEA NovoExpressTM.

Cellular uptake assays

After reviewing the results of Fav-SLNps cytotoxicity and autophagy, apoptosis, and cell cycle distribution assays, we investigated cellular uptake of the formula and free Fav. On day 1, 0.7×10^6 A549 human lung adenocarcinoma cells were seeded into a T25 flask and kept at 37 °C and 5% CO_2. On day 2, the medium was removed and replaced, and the cells were incubated with 300 μg/mL of Fav-SLNps or free Fav. After 6 or 24 h of incubation, cellular uptake was assessed via cell lysis, as described by Guntner et al.[52] At the end of the incubation, the amount of Fav was analysed with HPLC, as described previously, normalized to total protein, and expressed in μg/ml.[53]

Statistical analysis

One-way ANOVA, mean ± standard deviation, and unpaired two-tailed t-tests were used to analyse the data (IBM-SPSS Statistics, $P < 0.05$, version 22, USA). The IC50 plot explained the obtained results' nonlinear fit of "Normalize" and "Transform". The statistical value was calculated as the value of best fit in GraphPad Prism, version 9.

Results and discussion

Characterization of Fav-SLNps

The particle size and aerosol behaviour values of medication are important determinants of treatment effectiveness. Depending on their size, particles can be deposited through gravitational sedimentation, inertial impaction, or diffusion. Sedimentation occurs across the airways, and inertial impaction tends to occur during the first ten generations of the lung, where the airflow is turbulent, and the air velocity is high.[54] Any particles larger than 10 μm are deposited in the oropharyngeal region, and substantial deposition affects the larynx.[55,56] The large particles are then ingested and contribute little, if at all, to the therapeutic effect. Fluticasone propionate, for example, has low oral absorption, can be seen in a plasma levels.[54] Particles can be deposited in the alveoli and small airways when their diameter is between 1 and 5 μm. In pulmonary drug administration for systemic absorption, small particle-size aerosols are necessary to achieve medication peripheral penetration.[57] Particles less than 3 μm can reach the lower airways with approximately 80% probability and the alveoli with 50–60% probability.[58]

The particle size and aerosol behaviour results of the developed Fav-SLNp formulation have been published.[19] The geometric particle size distributions for Fav-SLNps and raw Fav were measured with dynamic light scattering. The mean diameter of Fav-SLNps and free Fav was 693.1 ± 40.3 nm and 1056.4 ± 181.2 nm, respectively—a size suitable for pulmonary applications as an inhaled formulation that might significantly improve therapeutic outcomes. The small particle size and large surface area may prevent negative adverse effects, decrease drug degradation, and enable targeted delivery.[8–15] The polydispersity index of Fav-SLNps and free Fav were 0.655 ± 0.020 and 0.451 ± 0.036, respectively. The zeta potential and surface charge of Fav-SLNps and free Fav were −13.3 ± 0.3 and −11.1 ± 0.2, respectively, thus indicating a slightly negative charge. Small particles with a net negative charge might be ionized by the carboxylic groups in compritol 888 (as a fatty acid).[59,60] Patel et al. have shown that particles with negative charges, rather than positive or neutral charges, tend to localize to the lymphatics.[61] Additionally, a negative or neutral nanoparticle surface charge for particles arriving at tumour sites may be more effective than a positive charge.[62] This evidence suggests promising potential of the Fav-SLNp formula in achieving greater treatment recovery and efficacy in lung cancer treatment.

In compliance with FDA industry standards, in terms of assessing aerosol particle appropriateness for administration to the airway, we used an ACI to examine the aerosol performance and size distribution of the nebulized Fav-SLNp formulation. An inhaler device can be used in vitro to determine the quality of the inhalable released product through a quality assurance procedure. Results are typically extrapolated to derive an estimate of in vivo deposition of the formulation into the lungs. Additionally, determining the location, depth of penetration, and accumulation within the lung mucosal membranes by using the TBN-NVS particle dimensions is critical.[63]

Figure 1 shows the characteristics of the nebulized Fav-SLNp formulation aerosol deposition behaviour in vitro, according to the ACI. Figure 1 shows Fav-SLNps deposition in ACI stages after nebulization in the nebulizer chamber, filter, throat, and ACI stages over the device-emitted dose. The log regression plot of this information was used to calculate the FPF, MMAD, and GSD. The percentage of FPF was identified as the drug mass percentage deposited from the third stage to the filter. The determined FPF and dose were 60.2 ± 1.7% and 332.3 ± 25.6 μg, respectively. The fine particle dose (μg ± SD) was 193.9 ± 13.1, the MMAD (μm ± SD) was 3.0 ± 0.4, and the GSD was 2.33 ± 0.25. These findings suggested good pulmonary Fav-SLNp delivery. The paths of these particles when they enter the deep lungs are positively affected by the aerodynamic surface. Optimized Fav-SLNps demonstrated high potential for deep accumulation, on the basis of the lung tissue FPF, MMAD, and GSD aerosol results. These findings suggested that customized Fav-SLNps may have strong pharmacological effectiveness against lung cancer.

In vitro bio-properties of Fav-SLNps

The goal of this study was to assess the aerosol behaviour of the Fav-SLN formulation in vitro and its appropriateness for administration to the lungs by nebulization. The treatment was also evaluated for its ability to prevent the increased proliferation of A549 cells; its effectiveness and appropriateness as a potential alternative lung cancer therapy were also examined.

Cell viability and cytotoxicity determination

The cytotoxicity and cell viability after treatment with the Fav-SLNs and free Fav formulation were examined in the A549 cell line through SRB assays. The influence of solid lipid nanoparticles on Fav cytotoxicity in lung cancer cells was assessed. To identify the suitable range of concentrations for lung delivery of the drug, as demonstrated in Figure 2(A & B),

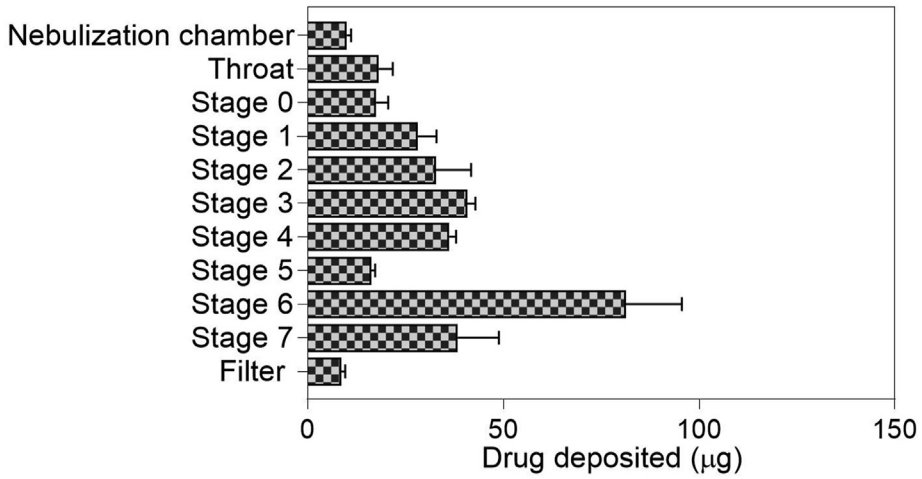

Figure 1: *In vitro* drug deposition of nebulized Fav-SLNps by the Andersen MKII Cascade Impactor (n = 3 ± S.D.).

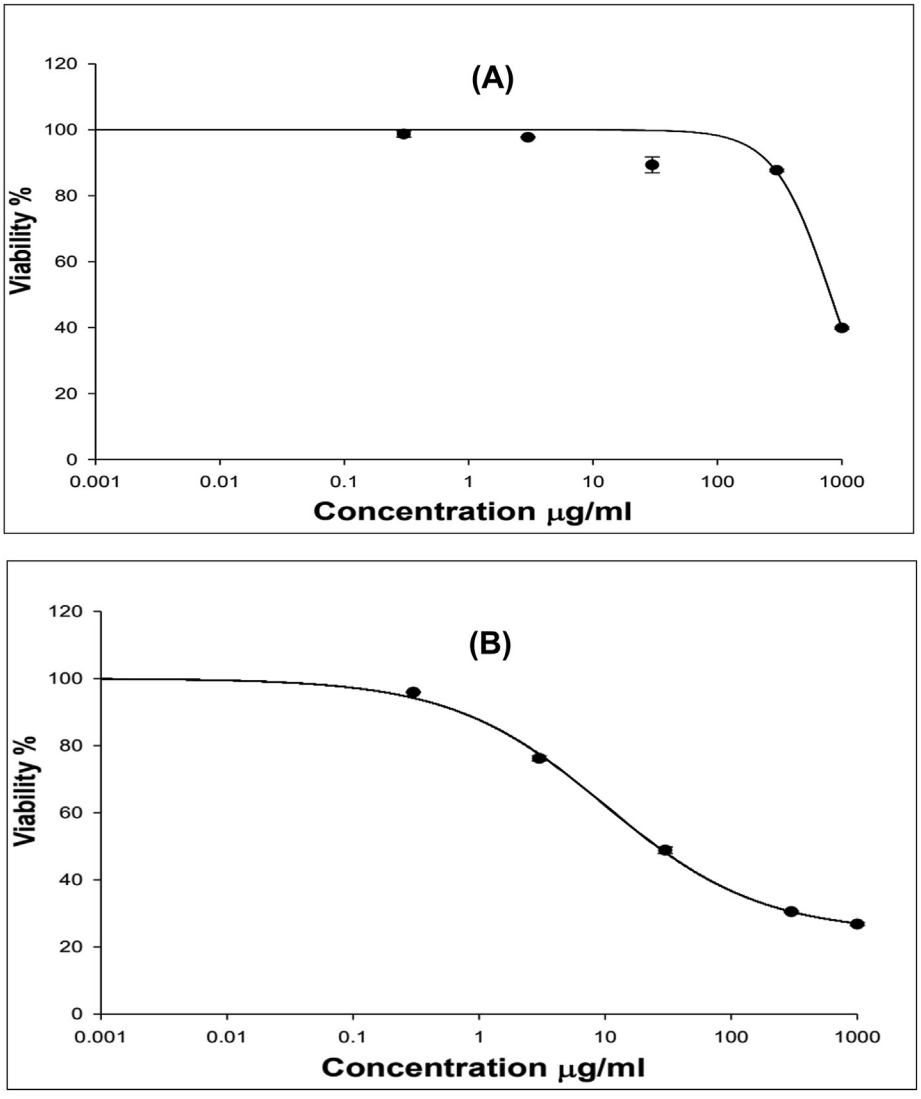

Figure 2: Cytotoxicity of (A) Fav-SLNps and (B) free Fav formulation toward A549 lung cancer cells (n = 3, mean ± SD).

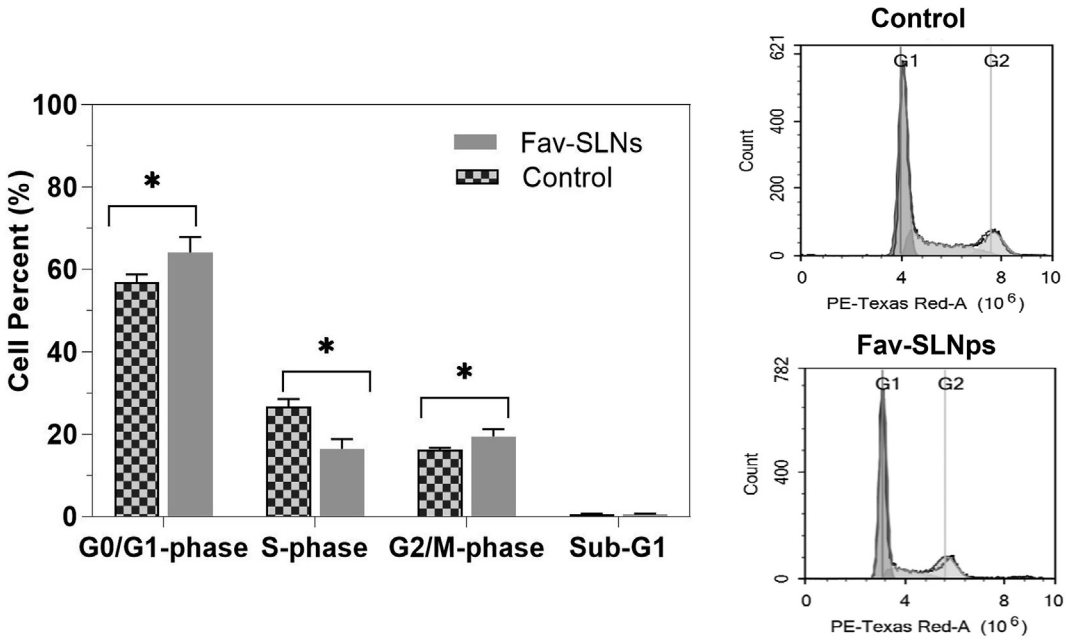

Figure 3: Effects of Fav-SLNp formulation on the cell cycle in A549 lung cancer cells (n = 3, mean ± SD).

we determined the toxicity of Fav-SLNps and free Fav in A549 non-small lung cancer cells. A549 cells were treated with increasing drug concentrations, ranging from 0.3 to 1000 µg/ml of Fav-SLNps for 72 h, to define the IC_{50}. Fav-SLNps and free Fav had an IC_{50} of 322.6 µg/ml and 10 µg/ml, respectively. The free Fav findings were consistent with those reported by Karakuş et al.[64] In addition, these findings suggested that Fav-SLNps are safe and non-toxic to cells; consequently, a lipid carrier might be favourable for Fav and could potentially be used to enhance the drug's effectiveness in A549 cells. A formulation of a drug with SLNps for the treatment of non-small cell lung cancer could improve the cell viability profile of the drug and decrease its toxicity. This finding was in line with those from prior studies indicating that Fav might be safe in the lungs.[19,65,66] This could be due to developing the formula using solid lipid nanoparticle techniques. Wang et al.[67] have found that formulating curcumin with solid lipid nanoparticles may have medicinal applications in lung cancer, and provides a unique technique for the creation of new anticancer drugs.[66] Another study has found similar results for cell viability and toxicity in A549 non-small cell lung cancer cells exposed to atorvastatin nanoparticles in vitro; this formula has been found to be safe and non-toxic at a 21 µg/mL concentration.[15] Fav might be able to be converted into an inhaled nano-formula as an efficient, safe and nontoxic therapy for lung cancer.

Influence of the Fav-SLNp formula on the cell cycle distribution

The DNA content was assessed with flow cytometry to investigate the influence of the Fav-SLNp formula on the cell cycle distribution of human lung adenocarcinoma cells after treatment with the therapies at the pre-determined IC_{50} for 24 h (Figure 3). Cell cycle evaluation can clarify Fav-SLNps' antiproliferative effects on the cell cycle phases of gap 1 (G1), synthesis (S), gap 2 (G2), mitosis (M), and resting (G0) phases.[67] The cell cycle is a four-stage process, consisting of M/G2, S, and G0/G1 phases, that cells undergo as they grow and divide.[68] Furthermore, measuring cell populations and cycles through apoptosis provides important indications regarding possible cell-killing.[69] In general, when cells were treated with Fav-SLNps (Figure 3), cells in G0/G1 phase markedly increased, from 56.87 ± 1.90% in the untreated sample to approximately 64.10 ± 3.80%. The Fav-SLNp formulation treatment, compared with the control, significantly altered the proliferative effects on G0/G1 phase after 1 day. The cell population in M/G2 phase increased from 16.16 ± 0.54% to 19.43 ± 1.78%, thus leading to considerable cell cycle arrest in M/G2 phase, as compared with that observed in untreated cells. This finding indicates that Fav-SLNp treatment caused cycle arrest at M/G2 and apoptosis to occur instantaneously in cells. This finding is important, because cell cycle arrest in M/G2 phase is considered a hallmark of anti-tumour activity.[70] Furthermore, the treatment of cells with the formula for 1 day caused no noticeable changes in the cell population (sub-G1) between the treated formulation and the control cells. Similarly, Tulbah et al. have found that an inhaled formulation of atorvastatin dry powder significantly inhibits cell cycle progression through either apoptosis or G2/M cell cycle arrest.[71] The formulation had anti-cancer properties with potential effects in lung cancer treatment.[71]

Effects of the Fav-SLNp preparation on A549 cell apoptosis

In tumour treatment, automatic cell death or apoptosis is considered the best target.[72,73] The fraction of cells that die by necrosis vs. apoptosis was determined in this analysis with Annexin V-FITC/PI labelling in combination with flow cytometry in A549 cells (Figure 4). Cells were treated with the predetermined IC_{50} of the Fav-SLNp formulation for 24 h before differential assessment of apoptosis/necrosis. Fav treatment for 24 h significantly stimulated necrotic cell death, with respect to that in untreated cells (Figure 4). In the necrotic phase, the ratio dose of Fav-SLNps (2.67 ± 0.49%)

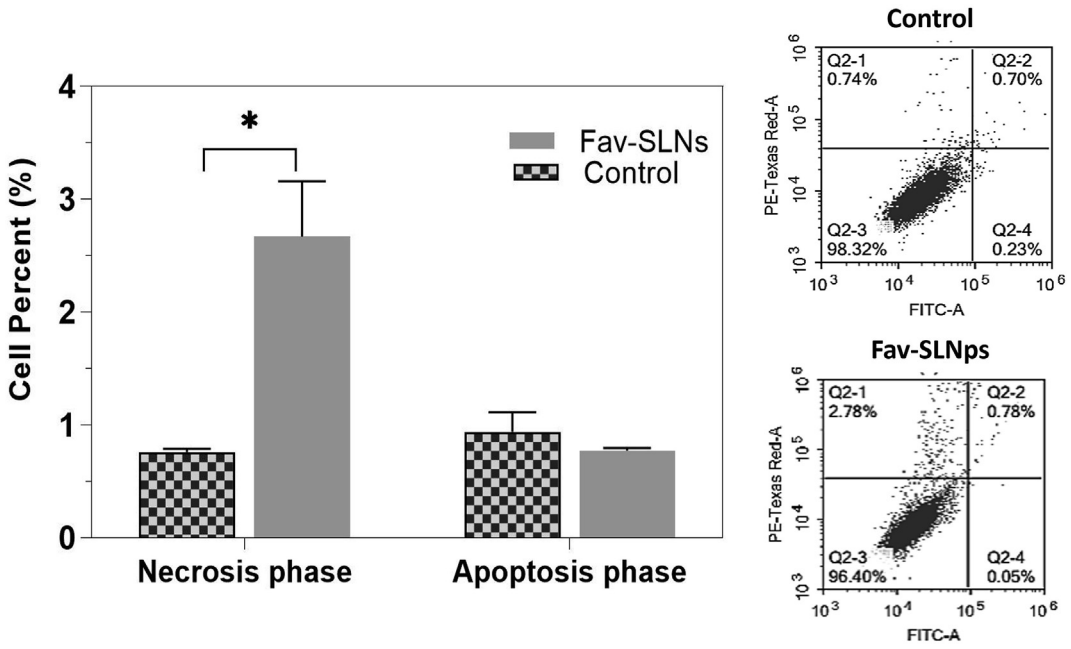

Figure 4: Effects of Fav-SLNp formulation on apoptosis and necrosis of A549 lung cancer cells (n = 3, mean ± SD).

was significantly increased (PI+ Annexin V − percentages) compared to the untreated cells (0.76 ± 0.03%). In addition, treatment with Fav-SLNps for 24 h induced necrotic cell death at a level 3.51-fold that in the control cells, possibly because of Fav's ability to trigger cell death in a variety of cell lines through either necrosis or apoptosis.[74] Inhibition of autophagy increases apoptosis in cancer cells with intact apoptotic signal transduction pathways.[75] Additionally, the formulation, in contrast to the control, did not induce apoptosis. Gowdhami et al. have indicated that cobalt (III) Schiff base complexes might serve as viable medications for lung cancer treatment through inducing A549 cell death apoptosis and necrosis.[76] Other research has discovered that grandiflorenic acid induces cytotoxicity and patterns of death associated with apoptosis in A549 lung tumour cell lines, and therefore plays a role in cell death; thus, the treatment had anti-cancer activity in lung cancer therapy.[77]

Influence of the Fav-SLNp formulation on the autophagy of A549 cells

Beyond apoptosis, autophagy-mediated programmed cell death is a major topic in science. Autophagy is a signalling pathway process that aids in the degradation of a wide range of cellular components.[78,79] In many biological settings, autophagy either restricts or accelerates the development of tumour cells.[80–82] Although the conditions under which autophagy serves as a major mechanism of cell survival or death remain unknown, one hypothesis is that autophagy suppression enhances apoptosis in cancer cells with intact apoptotic signalling pathways.[75] Herein, we examined the effect of the Fav-SLNp formulation on autophagy in A549 cells by using acridine orange lysosomal autophagy recognition dye paired with flow cytometry. In A549 cells, treatment with Fav-SLNps, compared with the control, significantly prevented autophagic cell death, which decreased from 11,519,364 to 1.45672333E+06 (Figure 5).

Cellular uptake assays

The assessment of Fav internalization by A549 cells will represent its internalization in the alveolar macrophage (AM) epithelium picture. At the 6 and 24 h time points, A549

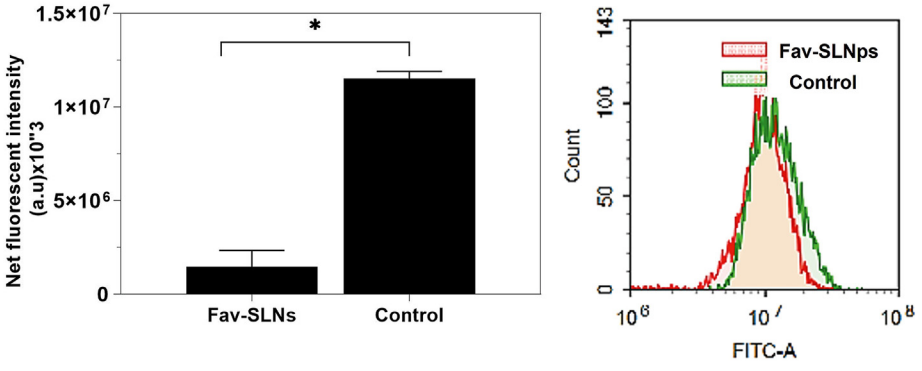

Figure 5: Effects of Fav-SLNp formulation on the autophagy mechanism of A549 lung cancer cells (n = 3, mean ± SD).

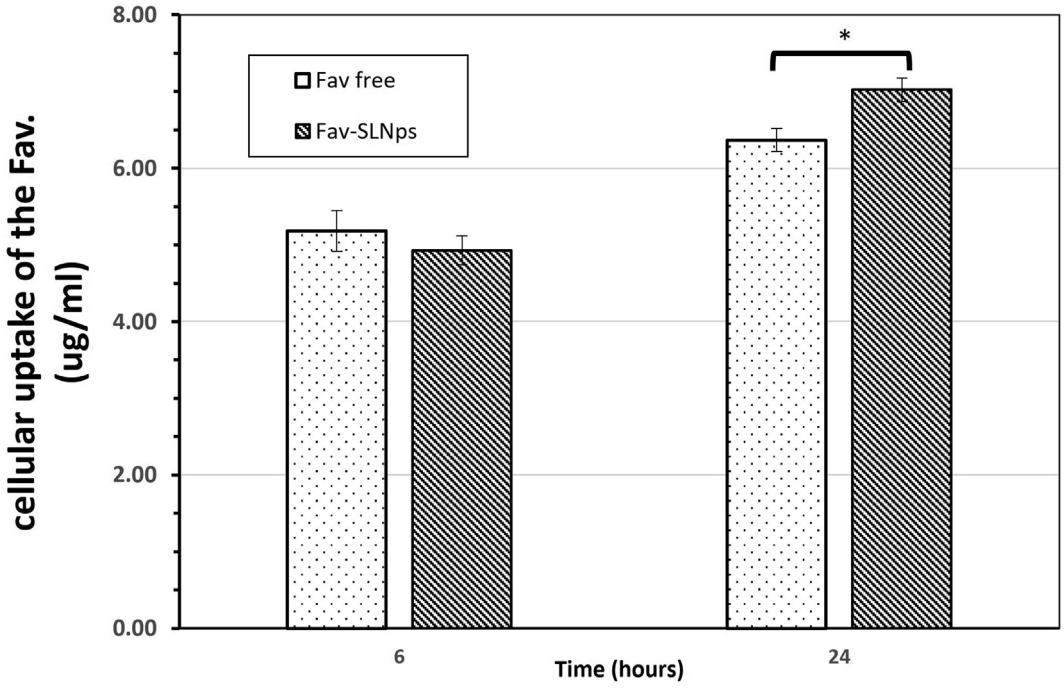

Figure 6: Cellular uptake efficacy of Fav-SLNps and free Fav in A549 cells. Results show three independent experiments (mean ± SD). Significant differences between medications are indicated by *P < 0.05.

cellular uptake of the Fav-SLNps and free Fav was investigated (Figure 6). Studies have revealed that smoke, dust, and air contamination are some of the environmental impurities that can reach the lungs and stimulate AMs under continuous exposure. AMs are considered the first line of the airways' intrinsic defence,[83–86] and their phagocytic activity and morphology can be altered in people continually exposed to environmental impurities.[87,88]

Thus, we added 300 μg/ml of Fav-SLNps and free Fav to A549 cells to evaluate the cellular internalization efficacy of both treatments. At 6 h, the cellular uptake was 4.93 μg/ml ± 0.19 and 5.18 μg/ml ± 0.26 for Fav-SLNps and free Fav, respectively, whereas after 24 h of cellular uptake, the internalization efficacy for Fav-SLNps and free Fav on A549 cells was 7.02 μg/ml ± 0.15 and 6.37 μg/ml ± 0.15, respectively. Interestingly, the data after 24 h of treatment revealed that the Fav-SLNp formulation had a better cellular internalization efficacy ($P > 0.05$) than free Fav.

Chono et al.[89] have found that SLNps have similar efficiency to that of liposomes in enhancing drug uptake into AMs, and the uptake increases with an increase in particle size from 100 to 1000 nm.[89] Thus, formulating Fav with SLNps might improve the cellular uptake activity of the drug. Phagocytosis and pinocytosis are different mechanisms through which particles or macromolecules can be taken up by cells, whereas in cells such as AMs, neutrophils, and monocytes, phagocytosis is the only mediated process.[90–93] Formulating Fav with SLNps increased the drug uptake into macrophages by 1.23 fold and may help avoid the adverse effects of the free drug. Thus, SLNps based on Fav may be a promising carrier for the effective treatment of lung cancer.

Conclusion

This study performed bio-characterization of Fav-SLNps in lung cancer treatment. The particle size and aerosol behaviour of the formula were suitable for inhalation of the medication. Additionally, Fav-SLNps at concentrations as high as 322.6 μg/ml were found to be safe and nontoxic toward A549 cells in vitro. The formulation had potential effects on anti-proliferative properties by increasing the cell population at the M/G2 and G0/G1 phases to 1.20- and 1.13-fold that in untreated cells, respectively. Necrosis in A549 cells was induced by Fav-SLNp treatment. Autophagy inhibition may be the mechanism underlying of the formula's effects on A549 cells. Additionally, the use of SLNps in the Fav formulation enhanced drug uptake into macrophages and therefore may help avoid the free drug's adverse effects. These findings suggest that Fav-SLNps may offer great potential for delivering drugs for the successful treatment of lung cancer. Future research will focus on testing the Fav-SLNp formula in an animal study to examine its toxicity, efficacy and pharmacokinetics in a realistic setting.

Source of funding

This research did not receive any specific grant from funding agencies in the public, commercial, or not-for-profit sectors.

Conflict of interest

The author have no conflict of interest to declare.

Ethical approval

The authors declare that no ethical approval was needed, and no animals or patients were studied.

References

1. Thandra KC, Barsouk A, Saginala K, Aluru JS, Barsouk A. Epidemiology of lung cancer. **Contemp Oncol 2021**; 25(1): 45–52. https://doi.org/10.1378/chest.123.1_suppl.21S.
2. Xu K, Zhang C, Du T, Gabriel ANA, Wang X, Li X, et al. Progress of exosomes in the diagnosis and treatment of lung cancer. **Biomed Pharmacother 2021**; 134:111111.
3. Alberg AJ, Brock MV, Ford JG, Samet JM, Spivack SD. Epidemiology of lung cancer: diagnosis and management of lung cancer: American College of Chest Physicians evidence-based clinical practice guidelines. **Chest 2013**; 143(5): e1S–e29S. https://doi.org/10.1378/chest.12-2345.
4. Caglar HB, Baldini EH, Othus M, Rabin MS, Bueno R, Sugarbaker DJ, et al. Outcomes of patients with stage III non-small cell lung cancer treated with chemotherapy and radiation with and without surgery. **Cancer 2009**; 115(18): 4156–4166.
5. Jonna S, Reuss JE, Kim C, Liu SV. Oral chemotherapy for treatment of lung cancer. **Front Oncol 2020**; 10: 793.
6. Lee MS, Dees EC, Wang AZ. Nanoparticle-delivered chemotherapy: old drugs in new packages. **Oncology 2017**; 31(3): 198–208.
7. Azarmi S, Roa WH, Lobenberg R. Targeted delivery of nanoparticles for the treatment of lung diseases. **Adv Drug Deliv Rev 2008**; 60(8): 863–875. https://doi.org/10.1016/j.addr.2007.11.006.
8. Ong HX, Benaouda F, Traini D, Cipolla D, Gonda I, Bebawy M, et al. In vitro and ex vivo methods predict the enhanced lung residence time of liposomal ciprofloxacin formulations for nebulisation. **Eur J Pharm Biopharm 2014**; 86(1): 83–89. https://doi.org/10.1016/j.ejpb.2013.06.024.
9. Tulbah AS, Pisano E, Scalia S, Young PM, Traini D, Ong HX. Inhaled simvastatin nanoparticles for inflammatory lung disease. **Nanomedicine 2017**; 12(20): 2471–2485. https://doi.org/10.2217/nnm-2017-0188.
10. Zhong Q, Bielski ER, Rodrigues LS, Brown MR, Reineke JJ, da Rocha SR. Conjugation to poly (amidoamine) dendrimers and pulmonary delivery reduce cardiac accumulation and enhance antitumor activity of doxorubicin in lung metastasis. **Mol Pharm 2016**; 13(7): 2363–2375. https://doi.org/10.1021/acs.molpharmaceut.6b00126.
11. Madni A, Batool A, Noreen S, Maqbool I, Rehman F, Kashif PM, et al. Novel nanoparticulate systems for lung cancer therapy: an updated review. **J Drug Target 2017**; 25(6): 499–512.
12. Estanqueiro M, Amaral MH, Conceição J, Lobo JMS. Nanotechnological carriers for cancer chemotherapy: the state of the art. **Colloids Surf B Biointerfaces 2015**; 126: 631–648.
13. Tulbah AS, Gamal A. Design and characterization of atorvastatin dry powder formulation as a potential lung cancer treatment. **Saudi Pharm, J 2021**; 29(12): 1449–1457.
14. Tulbah AS, Pisano E, Landh E, Scalia S, Young PM, Traini D, et al. Simvastatin nanoparticles reduce inflammation in LPS-stimulated alveolar macrophages. **J Pharm Sci 2019**; 108(12): 3890–3897. https://doi.org/10.1016/j.xphs.2019.08.029.
15. Tulbah AS. Inhaled atorvastatin nanoparticles for lung cancer. **Curr Drug Deliv 2022**. https://doi.org/10.2174/1567201819666220426091500.
16. Leong EW, Ge R. Lipid nanoparticles as delivery vehicles for inhaled therapeutics. **Biomedicines 2022**; 10(9): 2179. https://doi.org/10.3390/biomedicines10092179.
17. Kumar M, Jha A, Bharti K, Parmar G, Mishra B. Advances in lipid-based pulmonary nanomedicine for the management of inflammatory lung disorders. **Nanomedicine 2022**. https://doi.org/10.2217/nnm-2021-0389 (0).
18. Petros RA, DeSimone JM. Strategies in the design of nanoparticles for therapeutic applications. **Nat Rev Drug Discov 2010**; 9(8): 615–627.
19. Tulbah AS, Lee W-H. Physicochemical characteristics and in vitro toxicity/anti-SARS-CoV-2 activity of favipiravir solid lipid nanoparticles (SLNs). **Pharmaceuticals 2021**; 14(10): 1059.
20. Loo YS, Zahid NI, Madheswaran T, Azmi IDM. Recent advances in the development of multifunctional lipid-based nanoparticles for Co-Delivery, combination treatment strategies, and theranostics in breast and lung cancer. **J Drug Deliv Sci Technol 2022**:103300.
21. Bhatt S, Sharma J, Singh M, Saini V. Solid lipid nanoparticles: a promising technology for delivery of poorly water-soluble drugs. **Acta Pharm Sci 2018**; 56(3).
22. Sajadian SA, Ardestani NS, Esfandiari N, Askarizadeh M, Jouyban A. Solubility of favipiravir (as an anti-COVID-19) in supercritical carbon dioxide: an experimental analysis and thermodynamic modeling. **J Supercrit Fluids 2022**; 183:105539.
23. Shaik NB, Lakshmi PK. Formulation and evaluation of favipiravir proliposomal powder for pulmonary delivery by nebulization. **Int J Pharm Res Allied Sci 2022**; 11(2). https://doi.org/10.51847/4McfhPccXs.
24. Pilcer G, Amighi K. Formulation strategy and use of excipients in pulmonary drug delivery. **Int J Pharm 2010**; 392(1–2): 1–19. https://doi.org/10.1016/j.ijpharm.2010.03.017.
25. Kim CS, Duncan B, Creran B, Rotello VM. Triggered nanoparticles as therapeutics. **Nano Today 2013**; 8(4): 439–447.
26. Dhanani J, Fraser JF, Chan H-K, Rello J, Cohen J, Roberts JA. Fundamentals of aerosol therapy in critical care. **Crit Care 2016**; 20(1): 269. https://doi.org/10.1186/s13054-016-1448-5.
27. Patton JS, Platz RM. (D) Routes of delivery: case studies:(2) Pulmonary delivery of peptides and proteins for systemic action. **Adv Drug Deliv Rev 1992**; 8(2–3): 179–196. https://doi.org/10.1016/0169-409X(92)90002-8.
28. FAARC DRHPR. Nebulizers: principles and performance. **Respir Care 2000**; 45(6): 609.
29. Tulbah AS, Ong HX, Morgan L, Colombo P, Young PM, Traini D. Dry powder formulation of simvastatin. **Expet Opin Drug Deliv 2015**; 12(6): 857–868. https://doi.org/10.1517/17425247.2015.963054.
30. Alhaddad B, Smith F, Robertson T, Watman G, Taylor K. Patients' practices and experiences of using nebuliser therapy in the management of COPD at home. **BMJ Open Respir Res 2015**; 2(1):e000076.
31. Furuta Y, Gowen BB, Takahashi K, Shiraki K, Smee DF, Barnard DL. Favipiravir (T-705), a novel viral RNA polymerase inhibitor. **Antivir Res 2013**; 100(2): 446–454. https://doi.org/10.1016/j.antiviral.2013.09.015.
32. Wang M, Cao R, Zhang L, Yang X, Liu J, Xu M, et al. Remdesivir and chloroquine effectively inhibit the recently emerged novel coronavirus (2019-nCoV) in vitro. **Cell Res 2020**; 30(3): 269–271.
33. Shiraki K, Daikoku T. Favipiravir, an anti-influenza drug against life-threatening RNA virus infections. **Pharmacol Ther 2020**; 209:107512. https://doi.org/10.1016/j.pharmthera.2020.107512.
34. Joshi S, Parkar J, Ansari A, Vora A, Talwar D, Tiwaskar M, et al. Role of favipiravir in the treatment of COVID-19. **Int J Infect Dis 2021**; 102: 501–508.
35. Oestereich L, Lüdtke A, Wurr S, Rieger T, Muñoz-Fontela C, Günther S. Successful treatment of advanced Ebola virus infection with T-705 (favipiravir) in a small animal model. **Antivir Res 2014**; 105: 17–21.

36. Kim J, Seong R-K, Kumar M, Shin OS. Favipiravir and ribavirin inhibit replication of Asian and African strains of Zika virus in different cell models. **Viruses 2018**; 10(2): 72. https://doi.org/10.3390/v10020072.
37. Tanaka T, Kamiyama T, Daikoku T, Takahashi K, Nomura N, Kurokawa M, et al. T-705 (Favipiravir) suppresses tumor necrosis factor α production in response to influenza virus infection: a beneficial feature of T-705 as an anti-influenza drug. **Acta Virol 2017**; 61(1): 48–55. https://doi.org/10.4149/av_2017_01_48.
38. Boocock DJ, Patel KR, Faust GE, Normolle DP, Marczylo TH, Crowell JA, et al. Quantitation of trans-resveratrol and detection of its metabolites in human plasma and urine by high performance liquid chromatography. **J Chromatogr B 2007**; 848(2): 182–187.
39. Abdelrahim ME. Aerodynamic characteristics of nebulized terbutaline sulphate using the Andersen Cascade impactor compared to the next generation impactor. **Pharm Dev Technol 2011**; 16(2): 137–145. https://doi.org/10.3109/10837450903511194.
40. Pharmacopeia U. USP 39 NF 34. 2015.
41. Pharmacopoeia B. *British pharmacopoeia*; 2016.
42. Haghi M, Young PM, Traini D, Jaiswal R, Gong J, Bebawy M. Time- and passage-dependent characteristics of a Calu-3 respiratory epithelial cell model. **Drug Dev Ind Pharm 2010**; 36(10): 1207–1214. https://doi.org/10.3109/03639041003695113.
43. Marin L, Traini D, Bebawy M, Colombo P, Buttini F, Haghi M, et al. Multiple dosing of simvastatin inhibits airway mucus production of epithelial cells: implications in the treatment of chronic obstructive airway pathologies. **Eur J Pharm Biopharm 2013**; 84(3): 566–572. https://doi.org/10.1016/j.ejpb.2013.01.021.
44. Ong HX, Traini D, Bebawy M, Young PM. Epithelial profiling of antibiotic controlled release respiratory formulations. **Pharm Res 2011**; 28(9): 2327–2338. https://doi.org/10.1007/s11095-011-0462-1.
45. Allam RM, Al-Abd AM, Khedr A, Sharaf OA, Nofal SM, Khalifa AE, et al. Fingolimod interrupts the cross talk between estrogen metabolism and sphingolipid metabolism within prostate cancer cells. **Toxicol Lett 2018**; 291: 77–85. https://doi.org/10.1016/j.toxlet.2018.04.008.
46. Skehan P, Storeng R, Scudiero D, Monks A, McMahon J, Vistica D, et al. New colorimetric cytotoxicity assay for anticancer-drug screening. **J Natl Cancer Inst 1990**; 82(13): 1107–1112.
47. Tulbah AS, Ong HX, Lee W-H, Colombo P, Young PM, Traini D. Biological effects of simvastatin formulated as pMDI on pulmonary epithelial cells. **Pharm Res 2016**; 33(1): 92–101. https://doi.org/10.1007/s11095-015-1766-3.
48. Ong HX, Traini D, Ballerin G, Morgan L, Buddle L, Scalia S, et al. Combined inhaled salbutamol and mannitol therapy for mucus hyper-secretion in pulmonary diseases. **AAPS J 2014**: 1–12. https://doi.org/10.1208/s12248-014-9560-4.
49. Fekry MI, Ezzat SM, Salama MM, Alshehri OY, Al-Abd AM. Bioactive glycoalkaloids isolated from *Solanum melongena* fruit peels with potential anticancer properties against hepatocellular carcinoma cells. **Sci Rep 2019**; 9(1): 1–11. https://doi.org/10.1038/s41598-018-36089-6.
50. Bashmail HA, Alamoudi AA, Noorwali A, Hegazy GA, AJabnoor G, Choudhry H, et al. Thymoquinone synergizes gemcitabine anti-breast cancer activity via modulating its apoptotic and autophagic activities. **Sci Rep 2018**; 8(1): 1–11.
51. Mohamed GA, Al-Abd AM, El-Halawany AM, Abdallah HM, Ibrahim SR. New xanthones and cytotoxic constituents from *Garcinia mangostana* fruit hulls against human hepatocellular, breast, and colorectal cancer cell lines. **J Ethnopharmacol 2017**; 198: 302–312.
52. Guntner AS, Doppler C, Wechselberger C, Bernhard D, Buchberger W. HPLC-MS/MS shows that the cellular uptake of all-trans-retinoic acid under hypoxia is downregulated by the novel active agent 5-methoxyleoligin. **Cells 2020**; 9(9): 2048. https://doi.org/10.3390/cells9092048.
53. Lee W-H, Loo C-Y, Ong H-X, Traini D, Young PM, Rohanizadeh R. Synthesis and characterization of inhalable flavonoid nanoparticle for lung cancer cell targeting. **J Biomed Nanotechnol 2016**; 12(2): 371–386.
54. Lourenço RV, Cotromanes E. Clinical aerosols: I. Characterization of aerosols and their diagnostic uses. **Arch Intern Med 1982**; 142(12): 2163–2172. https://doi.org/10.1001/archinte.1982.00340250127019.
55. Heyder J. Particle transport onto human airway surfaces. **Eur J Respir Dis Suppl 1982**; 119: 29–50.
56. Morén F. *Aerosols in medicine: principles, diagnosis, and therapy*. Elsevier Science Limited; 1993.
57. Effros RM. Measurements of pulmonary epithelial permeability in vivo. **Am Rev Respir Dis 1983**; 127: S59–S65.
58. Patton JS. Mechanisms of macromolecule absorption by the lungs. **Adv Drug Deliv Rev 1996**; 19(1): 3–36.
59. Huang Zr, Hua Sc, Yang Yl, Fang Jy. Development and evaluation of lipid nanoparticles for camptothecin delivery: a comparison of solid lipid nanoparticles, nanostructured lipid carriers, and lipid emulsion. **Acta Pharmacol Sin 2008**; 29(9): 1094–1102. https://doi.org/10.1111/j.1745-7254.2008.00829.x.
60. Khan AA, Abdulbaqi IM, Abou Assi R, Murugaiyah V, Darwis Y. Lyophilized hybrid nanostructured lipid carriers to enhance the cellular uptake of verapamil: statistical optimization and in vitro evaluation. **Nanoscale Res Lett 2018**; 13(1): 1–16. https://doi.org/10.1186/s11671-018-2744-6.
61. Patel HM, Vaughan-Jones R. Assessment of the potential uses of liposomes for lymphoscintigraphy and lymphatic drug delivery failure of 99m-technetium marker to represent intact liposomes in lymph nodes. **Biochim Biophys Acta 1984**; 801(1): 76–86. https://doi.org/10.1016/0304-4165(84)90214-9.
62. Yuan YY, Mao CQ, Du XJ, Du JZ, Wang F, Wang J. Surface charge switchable nanoparticles based on zwitterionic polymer for enhanced drug delivery to tumor. **Adv Mater 2012**; 24(40): 5476–5480. https://doi.org/10.1002/adma.201202296.
63. Elkomy MH, El Menshawe SF, Kharshoum RM, Abdeltwab AM, Hussein RR, Hamad DS, et al. Innovative pulmonary targeting of terbutaline sulfate-laded novasomes for non-invasive tackling of asthma: statistical optimization and comparative in vitro/in vivo evaluation. **Drug Deliv 2022**; 29(1): 2058–2071. https://doi.org/10.1080/10717544.2022.2092236.
64. Karakuş A, Karakuş SÜ, Fatma U, Herdem Ü, Sude A, Özdemir F, et al. In vitro cytotoxic effects of some Covid-19 drugs on lung cancer cells. **Trak Univ J Nat Sci 2021**; 22(2): 173–177. https://doi.org/10.23902/trkjnat.901480.
65. Alotibi M. *Efficacy and safety of favipiravir for management of Covid-19: a retrospective study*. Jeddah–Saudi Arabia: King Abdulaziz University; 2021. 1/1443.
66. Wang P, Zhang L, Peng H, Li Y, Xiong J, Xu Z. The formulation and delivery of curcumin with solid lipid nanoparticles for the treatment of on non-small cell lung cancer both in vitro and in vivo. **Mater Sci Eng C 2013**; 33(8): 4802–4808. https://doi.org/10.1016/j.msec.2013.07.047.
67. Kuh HJ, Nakagawa Si, Usuda J, Yamaoka K, Saijo N, Nishio K. A computational model for quantitative analysis of cell cycle arrest and its contribution to overall growth inhibition by anticancer agents. **Jpn J Cancer Res 2000**; 91(12): 1303–1313. https://doi.org/10.1111/j.1349-7006.2000.tb00918.x.
68. Ravelli A. *Novel therapeutic approaches for the treatment of solid tumors*; 2019.
69. Pucci B, Kasten M, Giordano A. Cell cycle and apoptosis. **Neoplasia 2000**; 2(4): 291–299. https://doi.org/10.1046/j.1365-2184.2003.00267.x.

70. Xu X, Zhang Y, Qu D, Jiang T, Li S. Osthole induces G2/M arrest and apoptosis in lung cancer A549 cells by modulating PI3K/Akt pathway. **J Exp Clin Cancer Res 2011**; 30(1): 1−7.
71. Tulbah AS, Gamal A. Design and characterization of atorvastatin dry powder formulation as a potential lung cancer treatment. **Saudi Pharm J 2021**; 29(12): 1449−1457.
72. Abdelfadil E, Cheng Y-H, Bau D-T, Ting W-J, Chen L-M, Hsu H-H, et al. Thymoquinone induces apoptosis in oral cancer cells through p38β inhibition. **Am J Chin Med 2013**; 41(3): 683−696.
73. Hwang J-M, Ting W-J, Wu H-C, Chen Y-J, Tsai F-J, Chen P-Y, et al. KHC-4 anti-cancer effects on human PC3 prostate cancer cell line. **Am J Chin Med 2012**; 40(5): 1063−1071. https://doi.org/10.1142/S0192415X12500784.
74. Jafari M, Rezaei M, Kalantari H, Hashemitabar M. Determination of cell death induced by lovastatin on human colon cell line HT29 using the comet assay. **Jundishapur J Nat Pharm Prod 2013**; 8(4): 187−191. https://doi.org/10.17795/jjnpp-10951.
75. Ben Sahra I, Laurent K, Giuliano S, Larbret F, Ponzio G, Gounon P, et al. Targeting cancer cell metabolism: the combination of metformin and 2-deoxyglucose induces p53-dependent apoptosis in prostate cancer cells. **Cancer Res 2010**; 70(6): 2465−2475. https://doi.org/10.1158/0008-5472.Can-09-2782.
76. Gowdhami B, Manojkumar Y, Vimala R, Ramya V, Karthiyayini B, Kadalmani B, et al. Cytotoxic cobalt (III) Schiff base complexes: in vitro anti-proliferative, oxidative stress and gene expression studies in human breast and lung cancer cells. **BioMetals 2022**; 35(1): 67−85.
77. Fagundes TR, da Silva Bortoleti BT, Tomiotto-Pellissier F, Concato VM, Gonçalves MD, Arakawa NS, et al. Grandiflorenic acid from Wedelia trilobata plant induces apoptosis and autophagy cell death in breast adenocarcinoma (MCF7), lung carcinoma (A549), and hepatocellular carcinoma (HuH7. 5) cells lines. **Toxicon 2022**. https://doi.org/10.1016/j.toxicon.2022.08.006.
78. Pi H, Xu S, Zhang L, Guo P, Li Y, Xie J, et al. Dynamin 1-like-dependent mitochondrial fission initiates overactive mitophagy in the hepatotoxicity of cadmium. **Autophagy 2013**; 9(11): 1780−1800. https://doi.org/10.4161/auto.25665.
79. Pi H, Xu S, Reiter RJ, Guo P, Zhang L, Li Y, et al. SIRT3-SOD2-mROS-dependent autophagy in cadmium-induced hepatotoxicity and salvage by melatonin. **Autophagy 2015**; 11(7): 1037−1051. https://doi.org/10.1080/15548627.2015.1052208.
80. Fan TF, Bu LL, Wang WM, Ma SR, Liu JF, Deng WW, et al. Tumor growth suppression by inhibiting both autophagy and STAT3 signaling in HNSCC. **Oncotarget 2015**; 6(41): 43581−43593. https://doi.org/10.18632/oncotarget.6294.
81. Kimmelman AC. The dynamic nature of autophagy in cancer. **Genes Dev 2011**; 25(19): 1999−2010. https://doi.org/10.1101/gad.17558811.
82. Qin W, Li C, Zheng W, Guo Q, Zhang Y, Kang M, et al. Inhibition of autophagy promotes metastasis and glycolysis by inducing ROS in gastric cancer cells. **Oncotarget 2015**; 6(37): 39839. https://doi.org/10.18632/oncotarget.5674.
83. Dockery DW, Schwartz J, Spengler JD. Air pollution and daily mortality: associations with particulates and acid aerosols. **Environ Res 1992**; 59(2): 362−373. https://doi.org/10.1016/S0013-9351(05)80042-8.
84. Schwartz J, Dockery DW. Increased mortality in Philadelphia associated with daily air pollution concentrations. **Am Rev Respir Dis 1992**; 145(3): 600−604.
85. Dockery DW, Pope CA, Xu X, Spengler JD, Ware JH, Fay ME, et al. An association between air pollution and mortality in six US cities. **N Engl J Med 1993**; 329(24): 1753−1759. https://doi.org/10.1056/NEJM199312093292401.
86. Pope CA, Thun MJ, Namboodiri MM, Dockery DW, Evans JS, Speizer FE, et al. Particulate air pollution as a predictor of mortality in a prospective study of US adults. **Am J Respir Crit Care Med 1995**; 151(3): 669−674.
87. Byrne AJ, Mathie SA, Gregory LG, Lloyd CM. Pulmonary macrophages: key players in the innate defence of the airways. **Thorax 2015**; 70(12): 1189−1196.
88. Lohmann-Matthes M, Steinmuller C, Franke-Ullmann G. Pulmonary macrophages. **Eur Respir J 1994**; 7(9): 1678−1689.
89. Chono S, Tanino T, Seki T, Morimoto K. Influence of particle size on drug delivery to rat alveolar macrophages following pulmonary administration of ciprofloxacin incorporated into liposomes. **J Drug Target 2006**; 14(8): 557−566. https://doi.org/10.1080/10611860600834375.
90. Conner SD, Schmid SL. Regulated portals of entry into the cell. **Nature 2003**; 422(6927): 37−44.
91. Aderem A, Underhill DM. Mechanisms of phagocytosis in macrophages. **Annu Rev Immunol 1999**; 17(1): 593−623.
92. Mohning MP, Thomas SM, Barthel L, Mould KJ, McCubbrey AL, Frasch SC, et al. Phagocytosis of microparticles by alveolar macrophages during acute lung injury requires MerTK. **Am J Physiol Lung Cell Mol Physiol 2018**; 314(1): L69−L82.
93. Schneider DJ, Speth JM, Penke LR, Wettlaufer SH, Swanson JA, Peters-Golden M. Mechanisms and modulation of microvesicle uptake in a model of alveolar cell communication. **J Biol Chem 2017**; 292(51): 20897−20910. https://doi.org/10.1074/jbc.M117.792416.

How to cite this article: Tulbah AS. In vitro bio-characterization of solid lipid nanoparticles of favipiravir in A549 human lung epithelial cancer cells. J Taibah Univ Med Sc 2023;18(5):1076−1086.